

Symptom-based reliability analyses and performance assessment of corroded reinforced concrete structures

Hua-Peng Chen^{*1} and Nan Xiao^{2a}

¹*School of Engineering, University of Greenwich, Chatham Maritime, Kent, ME4 4TB, UK*

²*College of Civil Engineering & Architecture, Zhejiang University, Hangzhou 310058, China*

(Received November 22, 2013, Revised October 31, 2014, Accepted November 6, 2014)

Abstract. Reinforcement corrosion can cause serious safety deterioration to aging concrete structures exposed in aggressive environments. This paper presents an approach for reliability analyses of deteriorating reinforced concrete structures affected by reinforcement corrosion on the basis of the representative symptoms identified during the deterioration process. The concrete cracking growth and rebar bond strength evolution due to reinforcement corrosion are chosen as key symptoms for the performance deterioration of concrete structures. The crack width at concrete cover surface largely depends on the corrosion penetration of rebar due to the expansive rust layer at the bond interface generated by reinforcement corrosion. The bond strength of rebar in the concrete correlates well with concrete crack width and decays steadily with crack width growth. The estimates of cracking development and bond strength deterioration are examined by experimental data available from various sources, and then matched with symptom-based lifetime Weibull model. The symptom reliability and remaining useful life are predicted from the predictive lifetime Weibull model for deteriorating concrete structures. Finally, a numerical example is provided to demonstrate the applicability of the proposed approach for forecasting the performance of concrete structures subject to reinforcement corrosion. The results show that the corrosion rate has significant impact on the reliability associated with serviceability and load bearing capacity of reinforced concrete structures during their service life.

Keywords: reliability analysis; reinforcement corrosion; concrete cracking; bond strength; residual life

1. Introduction

The ability of concrete structures to fulfil their designed functions such as safety and reliability can be compromised because of performance deterioration. One of the major causes of performance degradation in reinforced concrete (RC) structures such as motorway bridges and marine structures is severe environments. During the service life of these RC structures, chlorides penetrate into the concrete cover and initiate chemical reactions, leading to reinforcement corrosion. Reinforcement corrosion consumes original steel rebar and generates expansive layer at the bond interface between reinforcement and the surrounding concrete cover. As corrosion

*Corresponding author, Senior Lecturer, E-mail: h.chen@greenwich.ac.uk

^aAssociate Professor

progresses, the expansive displacement at the bond interface generated by accumulating rust products causes tensile stress in the hoop direction within the concrete cover, leading to radial splitting cracks in the concrete and then bond strength deterioration of rebar. Consequently, the corrosion-induced concrete cracking and rebar bond strength deterioration can significantly affect the structural performance and eventually the remaining service life of the concrete structures.

Many investigations have been conducted during last decade regarding the influence of reinforcement corrosion and concrete cracking on the performance of concrete structures (Vidal *et al.* 2004, Pantazopoulou and Papoulia 2001, Chen and Alani 2013, Fang *et al.* 2013, Nepal *et al.* 2013, Sadeghi and Rezvani 2013). Research has been undertaken to assess the influence of reinforcement corrosion on concrete cracking (Mullard and Stewart 2011, Ortega *et al.* 2011, Chen and Xiao 2012, Kim *et al.* 2012) and to predict the remaining useful service life (Torres-Acosta and Martinez-Madrid 2003, Bhargava *et al.* 2007, Chen and Xiao 2011). Reliability analysis associated with limit states of a structural system is often utilised for assessing the safety of the system (Stewart and Rosowsky 1998). However, research on the time-dependent reliability analysis for concrete structures due to reinforcement corrosion is limited, with specific reference to the effect of concrete cracking on structural reliability. Therefore, there is a need to undertake research on how the monitored corrosion rate and concrete crack width could be utilised to evaluate structural reliability and estimate remaining service life.

Reliability analyses based on limit states of a structural system are generally used in structural design (Melchers 1999, Frangopol *et al.* 2008, Chen and Alani 2012). This approach, however, displays some limitations for the reliability analysis of existing structural systems, e.g., it usually ignores additional knowledge available from health monitoring, and it often neglects the performance deterioration over time. It is also unable to predict the future safety and performance of the structure (Straub and Faber 2005, Ceravolo *et al.* 2009, Chen and Bicanic 2010). Further investigations are therefore required on the reliability-based reassessment of structural systems, focusing on updating structural reliability from monitored data. The symptom-based reliability, originally proposed by Cempel *et al.* (2000), is more appropriate than the traditional time-based reliability for existing structural members and systems, as the monitoring process can provide useful data (symptoms) for further assessing current conditions and predicting future performance. The reliability analysis is thereafter enhanced by adopting continuously measured data in terms of geometry, material properties, structural deterioration, loading on the structure, and static and dynamic behaviour.

The paper deals with an effective method for evaluating symptom-based reliability and estimating the remaining useful life of deteriorating concrete structures subject to reinforcement corrosion. The concrete crack width and its associated bond strength evolution are selected as representative symptoms for the RC structures during the performance deterioration process. The concrete cracking growth is obtained from analytical solutions with consideration of realistic material properties. The bond strength evolution of rebar is evaluated on the basis of the development of concrete crack width. These predicted results are then adopted here as symptoms in the numerical simulation study for damage prognosis in order to predict the reliability associated with concrete cracking and rebar bond strength evolution.

2. Concrete cracking due to corrosion

The upcoming performance of RC structures exposed in aggressive environments depends on

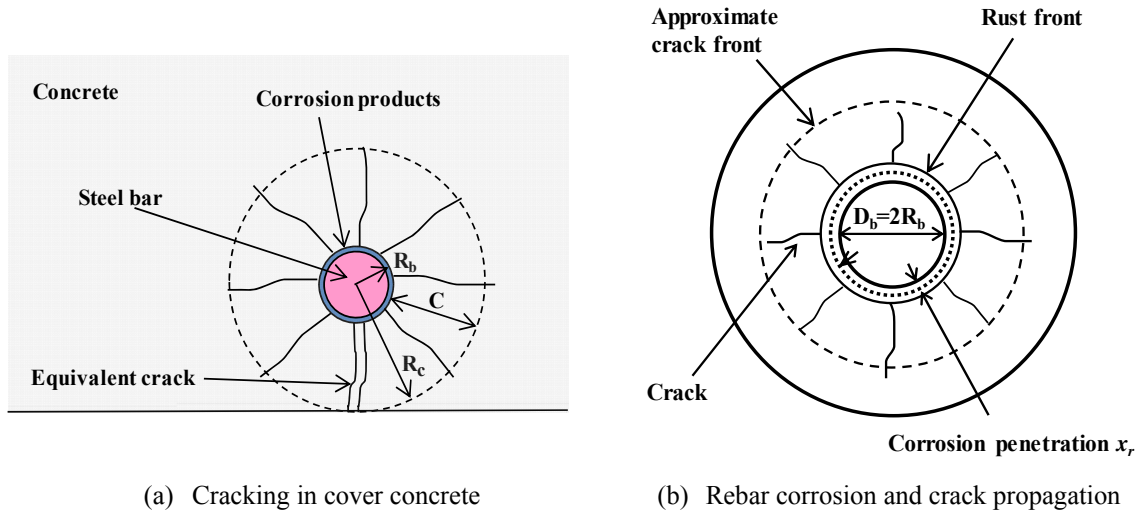


Fig. 1 Thick-walled cylinder model for cracking concrete

the corrosion-induced concrete cracking. The process of resistance degradation of RC structures affected by steel reinforcement corrosion is described in Fig. 1. The thick-walled cylinder indicated in Fig. 1 with internal radius of R_b , external radius of R_c and thickness C (clear concrete cover) is often used for investigating the influence of reinforcement corrosion on concrete performance. Three phases are considered in the process, i.e., crack initiation phase, crack propagation phase and residual life phase. The crack initiation phase ends at the time when the corrosion induced cracking initiates at the bond interface. After cracking occurs at the interface, the bond strength between steel reinforcement and the surrounding concrete starts decreasing, and the performance of the concrete structures deteriorates gradually. Due to further reinforcement corrosion, cracking propagates and widens in the concrete cover and then reaches an unacceptable level for the serviceability and load bearing capacity.

The built up of steel rebar corrosion products depends on the level of oxidation. Liu and Weyers (1998) reported that steel rebar may expand by as many as six times its original volume. The volume increase could be estimated if the mass of corrosion products and the mass of original steel consumed over time are available. The mass of rust products (kg/m) over time could be estimated from

$$M_r(t) = \left(2 \int_0^t \beta(\tau) d\tau \right)^{\frac{1}{2}} \quad (1)$$

where t is the time period of corrosion (year), and the function of the corrosion current $\beta(\tau)$ is related to the initial diameter of a steel rebar D_b (m) and the mean annual corrosion current per unit length at the surface area of the rebar i_{corr} (A/m²), defined here as

$$\beta(\tau) = 1.05 \times 10^{-2} \pi D_b i_{corr}(\tau) \quad (2)$$

The corrosion penetration rate x_r/R_b , defined as the ratio of the thickness of corrosion penetration over the original radius of rebar $R_b = D_b/2$, is expressed as

$$\frac{x_r}{R_b} = \frac{M_r(t)}{2\pi R_b^2 \rho_r \xi_r} \quad (3)$$

where ρ_r is density of corrosion rust with an approximate value of $\rho_r=3600 \text{ kg/m}^3$; ξ_r is volume expansion coefficient ranging from 2 to 4, determined by experiments. To accommodate the volume increase due to corrosion, the interface between steel rebar and the surrounding concrete is to displace by a prescribed quantity over time, which causes cracking in the cover concrete and consequently deteriorates the bond strength at the interface. The concrete cracking growth with time due to reinforcement corrosion was investigated by Chen and Alani (2013), where the equivalent crack width w over time t , defined as the cumulated crack width for a total number of cracks n_c over the concrete cover surface, is given by analytical solutions.

In the case before the crack front reaches concrete cover surface, no cracks appear on concrete cover surface, namely

$$w(t) = 0 \quad \text{for } 0 \leq t \leq T_c \quad (4)$$

The time to crack T_c is estimated, after ignoring the negligible time taken for completely filling the porous zone, from

$$M_r(T_c) = \left[1 + \frac{(l_0 - R_b)}{R_b} \frac{W_b}{W_{cr}} \right] R_b \frac{f_{ct}}{E} \frac{\pi D_b}{\alpha_m} \quad (5)$$

where E and ν are modulus of elasticity and Poisson's ratio of the concrete, respectively; f_{ct} is the tensile strength of the concrete; coefficient l_0 is characteristic length related to concrete properties; α_m is empirical coefficient taken as $\alpha_m=2.05 \times 10^{-4}$; W_{cr} is the coefficient when crack width becomes critical, in which the actual crack width w is normalized as dimensionless variable W , defined as $W=f_{ct}w/G_F$ where G_F is the fracture energy of concrete; the normalised crack width at the rebar surface W_b is expressed as

$$W_b = (1 + \nu) R_c (l_0 - R_c) \delta_{bc}(R_c, R_b) W_{cr} \quad (6)$$

and the crack width function $\delta_{bc}(R_c, r)$ related to radius r is defined as

$$\delta_{bc}(R_c, r) = \frac{(R_c - r)}{l_0(l_0 - R_c)(l_0 - r)} + \frac{1}{l_0^2} \ln \frac{R_c |l_0 - r|}{r |l_0 - R_c|} \quad (7)$$

In the case when the surrounding concrete is completely cracked within the concrete cover, the equivalent crack width in the concrete cover is expressed as

$$w(t) = a^c t^{1/2} - b^c \quad \text{for } T_c < t \leq T_{cr} \quad (8)$$

where a^c and b^c are coefficients for the cohesive concrete cracking propagation stage, defined as

$$a^c = 0.145 \alpha_m \frac{E}{f_t} \sqrt{\frac{i_{corr}}{\pi D_b}} \frac{1}{(l_0 - R_b)[1 - R_c(l_0 - R_c)\delta_{bc}(R_c, R_b)]} n_c W_{cr} \quad (9a)$$

$$b^c = \frac{\frac{R_b}{(l_0 - R_b)} + R_c(l_0 - R_c)\delta_{bc}(R_c, R_b)}{1 - R_c(l_0 - R_c)\delta_{bc}(R_c, R_b)} n_c W_{cr} \quad (9b)$$

The time taken for cracks to become critical in concrete T_{cr} is estimated from

$$M_r(T_{cr}) = l_0 \frac{f_t}{E} \frac{\pi D_b}{\alpha_m} \quad (10)$$

After the critical time T_{cr} , the discrete model is adopted and the cumulated crack width over the concrete cover surface is obtained from

$$w(t) = a^d t^{1/2} - b^d \quad \text{for } t > T_{cr} \quad (11)$$

where a^d and b^d are coefficients for the discrete concrete cracking stage, defined as

$$a^d = 0.145 \alpha_m \frac{\sqrt{\pi D_b i_{corr}}}{R_{cr}} \quad (12a)$$

$$b^d = \pi D_b \left(1 - \frac{R_b}{R_{cr}}\right) - n_c W_{cr} \quad (12b)$$

in which the front of corrosion rust R_{cr} is defined at the time when concrete cracks reach the critical value. The development of cracking in the concrete cover affected by reinforcement corrosion is analytically predicted, and will be used for evaluating the future performance of corroded concrete structures.

3. Bond strength affected by corrosion

Reinforcement corrosion can also affect the bond strength at the bond interface between rebar and the surrounding concrete. The loss of bond strength due to reinforcement corrosion can result in deteriorating the serviceability and reducing the load bearing capacity of concrete structures. Results from experimental investigations showed that typical bond failure was observed in the beams with corroded rebar (Bhargava *et al.* 2007). This is because the bond strength between rebar and the surrounding concrete was reduced due to corrosion and the pullout stress at the anchorage was increased until full anchorage was no longer maintained. The load bearing capacity such as bending resistance was determined by the bond strength of the rebar for anchorage rather than the yielding of fully bonded tensile rebar at failure. Therefore, the bond strength of rebar is a key parameter in evaluating the deterioration of structural load capacity due to reinforcement corrosion.

The bond strength of plain bars relies on adhesion and friction between rebar and the surrounding concrete. For deformed bars, bond strength depends on not only adhesion and friction and also mechanical interlocking between rebar and the surrounding concrete. Reinforcement corrosion impacts bond properties by changing the shape and angle of the ribs of deformed rebar. Corrosion also influences the mechanical interlocking between rebar and the surrounding concrete by reducing adhesion and frictional force due to the accumulation of corrosion products.

From the experimental investigations available, the contribution of bond strength from adhesion is relatively small and gradually vanishes as reinforcement corrosion progresses. The bond strength contributed from radial pressure at the bond interface reduces significantly when cracking appears on the surrounding concrete, decaying to zero when cover concrete crack width reaches the ultimate cohesive width. On the other hand, the bond strength contributed from the

confinement of the surrounding concrete is related to concrete crack width, as demonstrated in the experimental studies by Cairns *et al.* (2006), Law *et al.* (2011). It was found that bond strength correlates better with the crack width on the concrete cover, comparing with the corrosion level of steel reinforcement. From the analytical and experimental investigations by Giuriani *et al.* (1991) with ignoring adhesion contribution, the bond strength deterioration over time $\tau(t)$ can be expressed as a function of concrete crack width, namely

$$\tau(t) = \frac{1}{1 + \lambda_1 w(t)/D_b} \tau_{u0} + \frac{1}{1 + \lambda_2 w(t)/D_b} \mu_0 [k_1 \sigma_{st}(t) + k_2 \sigma_{rc}(t)] \quad (13)$$

where τ_{u0} is the ultimate bond strength of the rebar without concrete cracking; λ_1 , λ_2 and μ_0 are coefficients associated with concrete properties but independent of D_b , determined by experiments; k_1 is the stirrup index of confinement defined as the ratio of the global cross-sectional area of the stirrup legs over the area of rebar in the splitting plane; k_2 is the concrete index of confinement defined as the ratio of the net area of the concrete in the splitting plane over the area of rebar in the splitting plane. The bond strength contribution of the confining action is generated from both the steel stirrup stress σ_{st} and the cracked concrete stress σ_{rc} .

In order to consider the influence of reinforcement corrosion on the confinement contribution from the steel stirrups and the surrounding cracked concrete, the original relations given in Giuriani *et al.* (1991) are modified here, respectively, as

$$\sigma_{st}(t) = \frac{A_{st}}{D_r \Delta z} E_{st} \sqrt{\frac{a_2 w^2(t)}{\alpha_s^2 d_{st}^2} + \frac{a_1 w(t)}{\alpha_s d_{st}^2} + a_0} \quad (14a)$$

$$\sigma_{rc}(t) = \frac{2C}{D_r} \frac{1 - w(t)/w_{cr}}{1 + k_c w(t)/d_a} f_{ct} \quad (14b)$$

where A_{st} is the cross-sectional area of stirrup leg; D_r is residual diameter of rebar due to corrosion; Δz is the spacing of stirrup; E_{st} is the modulus of elasticity of steel stirrups; Coefficients a_0 , a_1 and a_2 are related to trilateral local bond-slip law of stirrups determined by experiments; α_s is the shape factor of stirrup; d_{st} is the diameter of stirrup leg; k_c is the constant determined from experiments; d_a is maximum aggregate size of concrete. The concrete crack width $w(t)$ over time depends on reinforcement corrosion level and can be estimated by the method described in the previous section.

The bond strength of rebar decreases as reinforcement corrosion develops, but maintains a small value at relatively large crack width due to confinement from steel stirrups around the rebar. In order to evaluate the bond strength deterioration more appropriately, normalised bond strength is now introduced as

$$\eta(t) = \frac{\tau(t)}{\tau_{u0}} = \frac{1}{1 + \lambda_1 w(t)/D_b} + \frac{s(t)}{1 + \lambda_2 w(t)/D_b} \quad (15)$$

where $\eta(t)$ is bond strength ratio over time t , and $s(t)$ is associated with steel stirrup stress and the cracked concrete stress defined as $s(t) = \mu_0 [k_1 \sigma_{st}(t) + k_2 \sigma_{rc}(t)] / \tau_{u0}$. In the cases when the confining stresses in concrete and stirrups are not available, the relation of rebar bond strength with concrete cracking could be further simplified as

$$\eta(t) = \frac{1}{1 + \lambda w(t)/D_b} \quad (16)$$

where λ is coefficient determined by experiments.

4. Symptom-based reliability analysis

The symptom-based reliability was proposed by Cempel *et al.* (2000) initially, and recently further extended to be used for civil engineering structures (Ceravolo *et al.* 2009). In symptom-based system performance evaluation, the reliability is assumed to be dependent of measurable quantities, i.e., symptom. The system and its components fail to meet the designed requirements when a symptom exceeds a given limit value S_l . Symptom reliability $R(S)$ for a critical system in operation can be defined as the probability associated with a symptom S , where a system classified as in good condition ($S < S_l$) will be in operation with the measured symptom value below the failure value $S < S_b$, expressed here as

$$R(S) = P(S < S_b \mid S < S_l) = \int_s^\infty f_s dS \quad (17)$$

From above, it can be seen that the symptom reliability $R(S)$ can be expressed by the integral of the symptom's distribution probability density f_s . The symptom hazard function $h(S)$, depending on the symptom of condition S , is defined in Lawless (1982) as

$$h(S) = -\frac{d \ln R(S)}{dS} = -\frac{1}{R(S)} \frac{dR(S)}{dS} \quad (18)$$

Consequently, the symptom reliability $R(S)$ is calculated from the symptom hazard function as

$$R(S) = \exp\left(-\int_0^S h(\theta) d\theta\right) \quad (19)$$

For RC structures subjected to aggressive environments, the corrosion-induced cracking of the cover concrete and the loss of bond strength can be used for representative symptoms to evaluate the symptom-based reliability. The reliability of the corroded RC structures is then predicted on the basis of the evolution of selected symptoms over time.

In general, there are two basic system lifetime distribution models used in symptom based reliability analysis, Weibull and Frechet models. The Weibull model is often used for structural capacity deterioration caused by structural damage. In this study, the Weibull model adopted for concrete cracking and bond strength deterioration is assumed as

$$\frac{S}{S_l} = \alpha \left[-\ln\left(1 - \frac{t(S)}{t_b}\right) \right]^{1/\gamma} \quad (20)$$

where $\alpha > 0$ is the scale parameter; $\gamma > 0$ is the shape parameter; the initial symptom is $S_0 = \alpha S_l$ in which S_l is an allowable limit for concrete crack width or bond strength loss; t_b is the design life of the RC structure. The associated symptom hazard function for the Weibull model is expressed as

$$h(S) = \frac{\gamma}{\alpha S_l} \left[\frac{S}{\alpha S_l} \right]^{\gamma-1} \quad (21)$$

and the reliability associated with the selected symptom is given by

$$R(S) = \exp\left[-\left(\frac{S}{\alpha S_i}\right)^\gamma\right] \quad (22)$$

Consequently, the remaining useful life for the reinforced structures can be predicted from

$$t_{rul}(S) = R(S)t_b = \exp\left[-\left(\frac{S}{\alpha S_i}\right)^\gamma\right]t_b \quad (23)$$

In the case where the measured data are different from the expected value, a logistic vector L_i is introduced to adjust the symptom based reliability analyses. For RC structures, the logistic vector may contain information such as geometry, loads, environments and material properties. The symptom hazard function $h(S(L))$ is now assumed to have general expression as a function of the logistic vector, expressed here as

$$h(S, L) = h_0(S)g(L) \quad (24)$$

where $h_0(S)$ indicates the primary hazard function, and $g(L)$ is any function satisfying $g(L_0)=1$. The modified symptom reliability can now be calculated from

$$R(S, L) |_{L_0+\Delta L} = R_0(S, L_0) \left\{ 1 + \Delta L^T \frac{\partial g}{\partial L} \ln(R_0(S, L_0)) \right\} \quad (25)$$

Here, the primary symptom reliability $R_0(S, L_0)$ associated with initial logistic vector L_0 is defined as

$$R_0(S, L_0) = \exp \left\{ - \int_0^S h_0(\theta) g(L_0) d\theta \right\} \quad (26)$$

When the hazard function is proportional to the single measured system symptom S_m , the hazard function may be expressed as

$$h(S, L) = h_0(S)L = h_0(S) \frac{S_m}{S_0} \quad (27)$$

The modified symptom reliability is now rewritten here as

$$R(S, L) |_{L_0+\Delta L} = R_0(S) \left\{ 1 + \frac{\Delta S}{S_0} \ln(R_0(S)) \right\} \quad (28)$$

When the difference $\Delta S = S_m - S > 0$ the symptom reliability decreases, while $\Delta S < 0$ the system reliability increases.

5. Numerical example

A steel reinforced concrete structure exposed to an aggressive environment with a design service life of 75 years is now utilised to demonstrate the applicability of the proposed reliability analysis approach. The reinforcing steel bars of a diameter of 12mm are embedded into concrete structural elements with an average clear cover thickness of 39mm. The concrete has a specified

compressive strength of 34.5 MPa. The critical crack width w_{cr} is the cohesive crack opening at zero residual strength, evaluated from the fracture energy and the maximum aggregate size with a value of 0.1 mm. The total crack number n_c is calculated from $n_c=2\pi R_c/L_c$ and estimated to be 4 for the given material properties.

In order to predict concrete crack growth, a mean annual corrosion current $i_{corr}=1.0 \mu A/cm^2$, corresponding to a moderate corrosion risk, is adopted in calculations. The time period for the crack initiation is 0.368year, which is very short comparing the service life of the structure. Cracks then propagate from the bond interface to the concrete cover surface. The time taken for crack front to reach the cover surface (T_c) mainly depends on corrosion penetration x_r and concrete tensile strength f_{ct} , estimated as 1.13year. At the time when $T_{cr}=16.40year$, the crack width within the surrounding concrete cover becomes critical. After the critical time T_{cr} cracks in the concrete open further and reach a value of 0.87 mm at the service life of 60 years. In order to investigate influence of corrosion rate on concrete cracking growth and bond strength deterioration, various values of corrosion rate are adopted to undertake the reliability analyses of the corroded RC structures.

5.1 Concrete cracking as symptom

In order to validate the results predicted by the proposed approach, the obtained crack width over time is plotted in Fig. 2 as a function of corrosion penetration rate (x_r/r_0). The predicted results are then compared with the experimental data from various sources in the study by Torres-Acosta and Martinez-Madrid (2003). It is found that the predicted results for the crack growth in the surrounding concrete cover due to reinforcement corrosion agree well with the experimental data available.

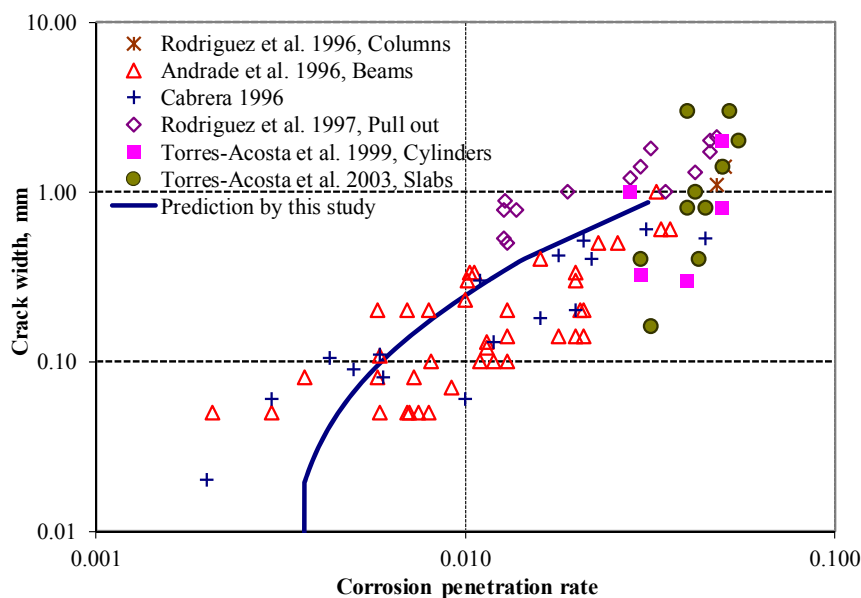


Fig. 2 Concrete crack width as a function of corrosion penetration rate, compared with the experimental data available from Torres-Acosta and Martinez-Madrid (2003)

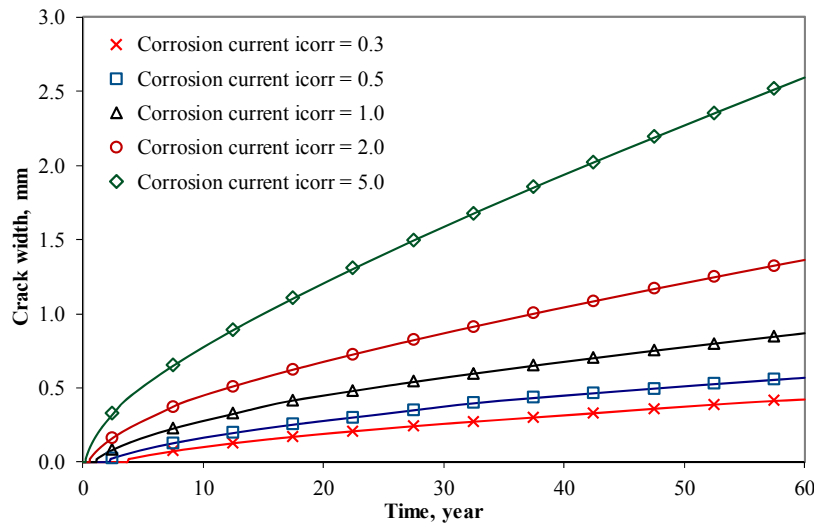


Fig. 3 Concrete crack widths at cover surface over time t for various corrosion rates

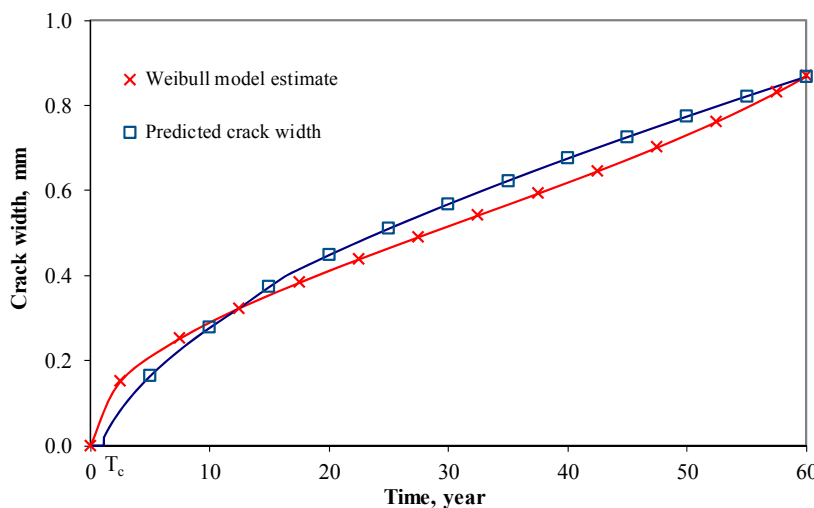


Fig. 4 Comparison of concrete cracking growth by analytical results with the predictions by Weibull model in the case with corrosion rate of $1.0 \mu A/cm^2$

In order to investigate the effect of corrosion current i_{corr} on concrete crack evolution, various values of corrosion rate ranging from 0.3 to $5.0 \mu A/cm^2$ are adopted to predict the crack width at the concrete cover surface, as shown in Fig. 3. The obtained results indicate that the crack width at the concrete cover surface over time largely depends on the corrosion rate i_{corr} . The predicted value of crack width is tripled when corrosion rate increases from 1.0 to $5.0 \mu A/cm^2$.

Fig. 4 gives results for lifetime evolution of corrosion-induced concrete cracking predicted by Weibull model, which are compared with the analytical results obtained from the proposed approach, where the case with corrosion rate of $1.0 \mu A/cm^2$ is considered. The scale parameter $\alpha=0.7$ and shape parameter $\gamma=2.2$ are determined to best match the analytical predictions with the

estimates from Weibull model. Similarly, the scale parameter α is taken as 0.34, 0.45, 1.12, and 2.1 for corrosion rates of 0.3, 0.5, 2, 5 $\mu\text{A}/\text{cm}^2$, respectively, with the same shape parameter $\gamma=2.2$ for all corrosion rates.

The symptom reliability associated with concrete cracking for various corrosion rates are plotted in Fig. 5. The reliability decreases with time due to the growth of corrosion-induced concrete cracking. As the corrosion rate increases the symptom reliability reduces significantly. This confirms the corrosion-induced concrete crack is appropriate for the dominant symptom responsible for performance deterioration.

Fig. 6 shows the results for the symptom hazard function associated with concrete cracking for various corrosion rates. As expected, the associated symptom hazard increases with time gradually. The hazard function however is significantly affected by the corrosion rate, increasing about three times as corrosion rate increases from 1.0 to 5.0 $\mu\text{A}/\text{cm}^2$.

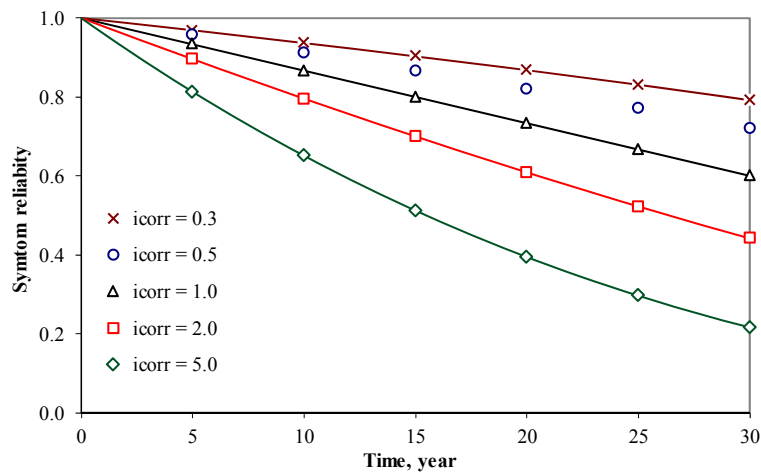


Fig. 5 Symptom reliability associated with concrete cracking over time t for various corrosion rates

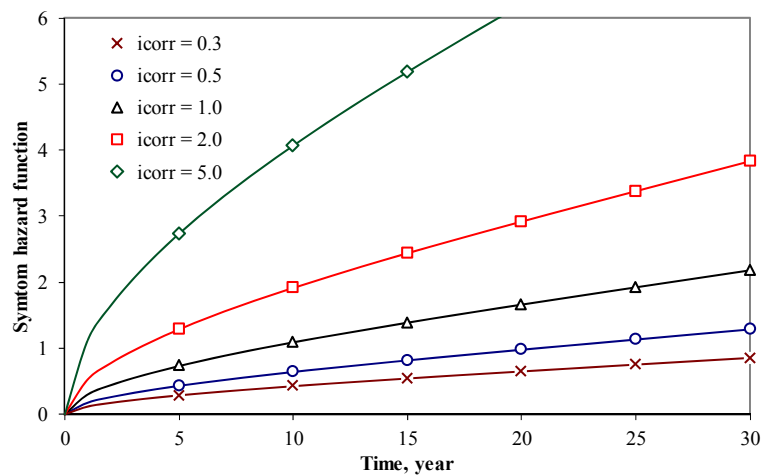


Fig. 6 Symptom hazard function associated with concrete cracking over time t for various corrosion rates

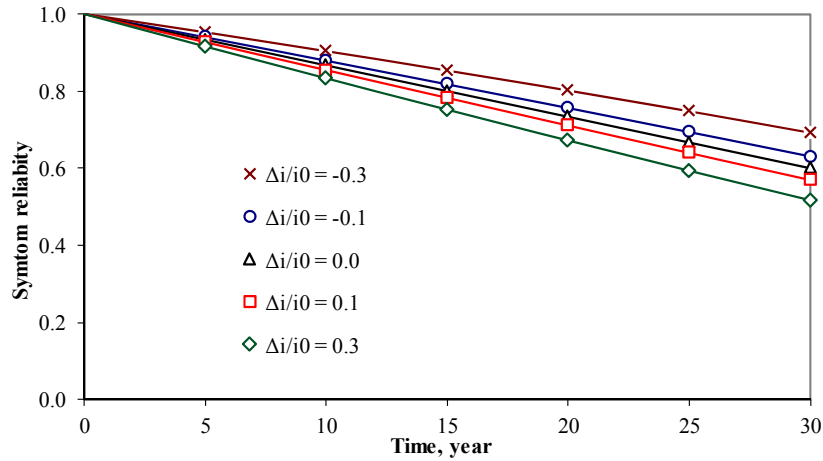


Fig. 7 Influence of field corrosion rate measurements on symptom reliability associated with concrete cracking

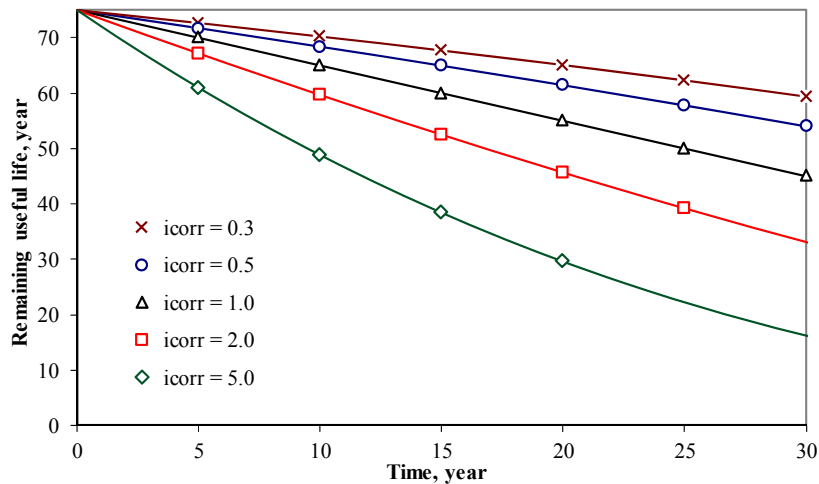


Fig. 8 Estimated remaining useful lifetimes associated with concrete cracking over life time for various corrosion rates

When the real corrosion rate measurements are different from the value used in structural design (i_0), the symptom reliability will be affected by the difference (Δi). The results in Fig. 7 show the symptom reliability associated with concrete cracking decreases when the monitored corrosion rate exceeds the design value. On the other hand, the reliability increases when the monitored corrosion rate is below the design value. This again shows that corrosion rate has significant impact on symptom reliability associated with concrete cracking, and the associated reliability needs to be adjusted on the basis of real corrosion rate measurements in operational environments.

The remaining useful life is then predicted from the estimated symptom reliability, as shown in Fig. 8. From results, it can be seen that the corrosion rate has a significant influence on the

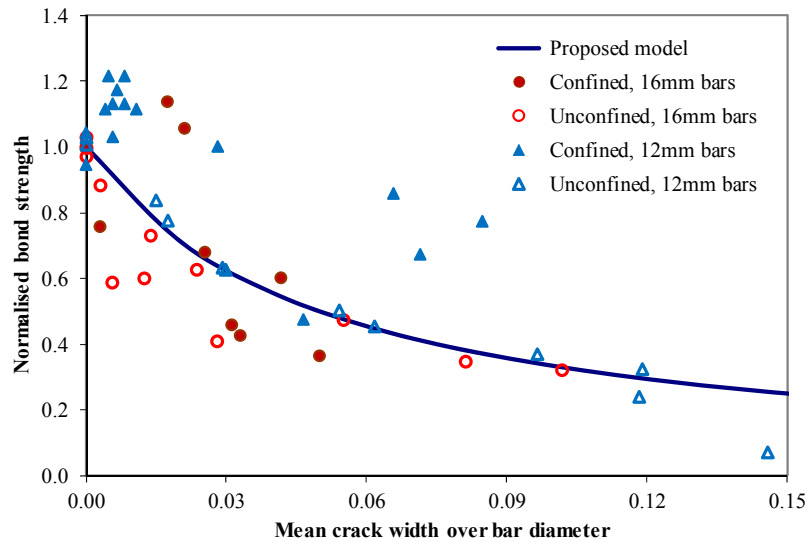


Fig. 9 Predicted bond strength ratio as a function of the ratio of concrete crack width over rebar diameter, compared with experimental results by Law *et al.* (2011) with or without stirrups

remaining useful life, reducing from 45 year for corrosion rate of $1.0 \mu\text{A}/\text{cm}^2$ to 16 year for corrosion rate of $5.0 \mu\text{A}/\text{cm}^2$ after 30 year service of the structure.

5.2 Bond strength as symptom

Concrete crack width at the cover surface is a measurable parameter on site and can also be predicted from the proposed analytical method. Experimental investigations show that bond strength evolution correlates better with concrete crack width, comparing with corrosion penetration level. In this study, bond strength evolution is estimated from the simplified relation in Eq. (16) as a function of concrete crack width over time, where coefficient λ is taken as 20. These predictions are then examined by the experimental results by Law *et al.* (2011), where both cases with or without steel stirrups were tested. From the results in Fig. 9, the predictions from the simplified relation match well with the experimental results. The bond strength of the corroded rebar is significantly affected by concrete crack width, starting decreasing when cracking initiates at concrete surface and then decaying to a small value as concrete crack width becomes relatively large.

The effects of corrosion rate on the bond strength of rebar are investigated in Fig. 10, where various values of mean annual corrosion current per unit length, ranging from $i_{\text{corr}}=0.3$ to $5.0 \mu\text{A}/\text{cm}^2$ are considered. The results show that bond strength deterioration largely depends on the corrosion rate at rebar surface. The bond strength can be reduced to half if corrosion rate increases from 1.0 to $5.0 \mu\text{A}/\text{cm}^2$.

The life time evolution of bond strength of rebar in the concrete structure can also be matched well with Weibull model. Fig. 11 plots the obtained bond strength deterioration over time together with the estimates from Weibull model. It is found that the obtained results are in good agreement with the estimates from Weibull model, giving the shape parameter $\gamma=2.75$ and the scale parameter $\alpha=0.82$ for the case with corrosion rate of $1.0 \mu\text{A}/\text{cm}^2$. The shape parameter appears the same for

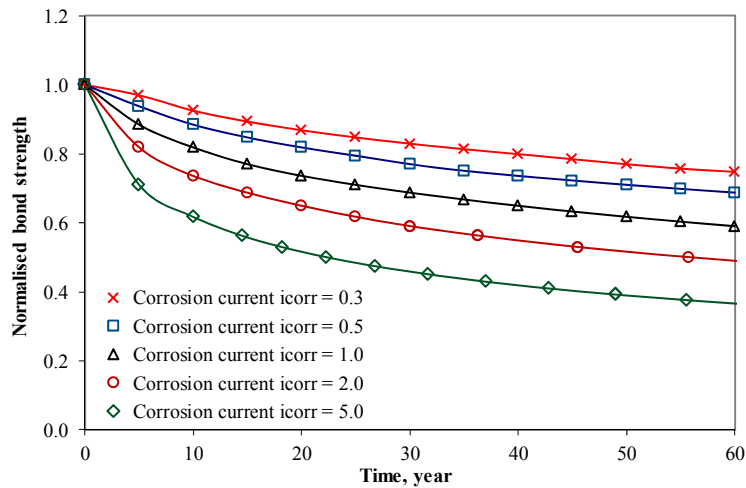


Fig. 10 Normalised bond strength evolution over time t for various corrosion rates

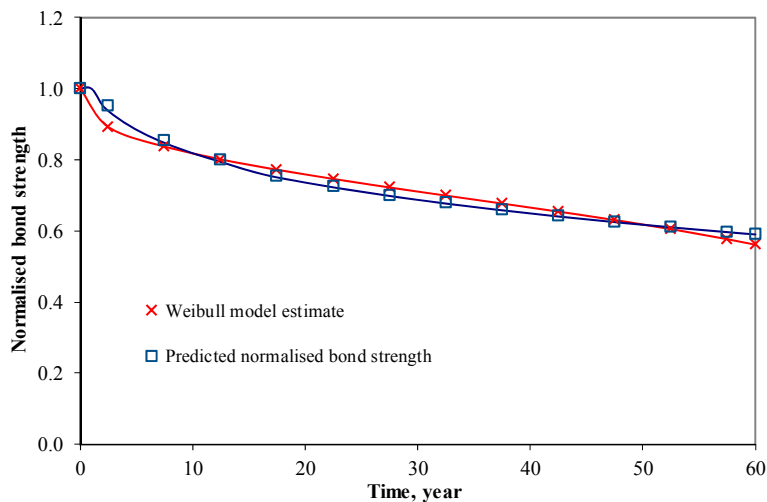


Fig. 11 Comparison of proposed bond strength evolution with Weibull model predictions in the case with corrosion rate of $1.0 \mu\text{A}/\text{cm}^2$

various corrosion rates, while the scale parameter is taken as 0.45, 0.61, 1.21 and 1.75 for the cases with corrosion rates of 0.3, 0.5, 2.0 and $5.0 \mu\text{A}/\text{cm}^2$, respectively.

From the determined Weibull model for bond strength evolution, the associated symptom reliability can now be calculated for various corrosion rates, as shown in Fig. 12. From the obtained results, the associated reliability affected by reinforcement corrosion decreases with time, reducing from bond strength ratio of 1.0 initially to a value of 0.2 at time of 60 year in the case with corrosion rate of $1.0 \mu\text{A}/\text{cm}^2$. This reduced value can be considered as unacceptable reliability for the load bearing capacity of the RC structure. As expected, the associated reliability is significantly affected by corrosion rate. The associated reliability drops to a half value when corrosion rate increases from 1.0 to $5.0 \mu\text{A}/\text{cm}^2$.

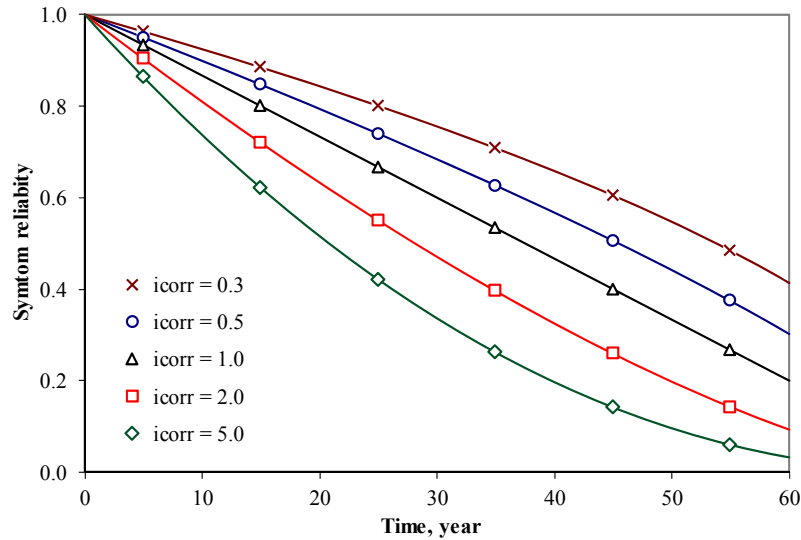


Fig. 12 Symptom reliability associated with bond strength evolution over time t for various corrosion rates

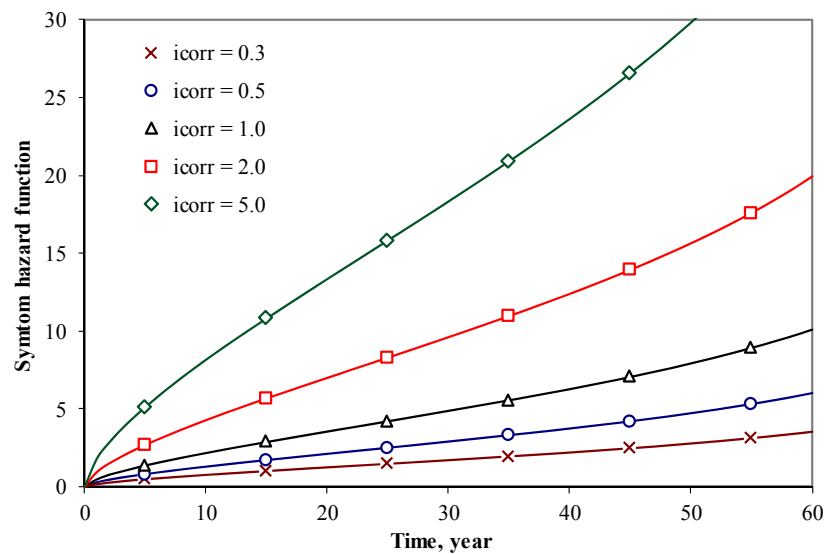


Fig. 13 Symptom hazard function associated with bond strength evolution over time t for various corrosion rates

Fig. 13 shows the results for symptom hazard function associated with bond strength evolution over time, where corrosion rates ranging from 0.3 to 5.0 $\mu\text{A}/\text{cm}^2$ are considered. Due to the deterioration of bond strength of rebar in the concrete, the associated hazard steadily increases with time, and the hazard rate becomes larger as the life time of the concrete structure increases. Here again, the larger corrosion rate at the rebar surface can cause higher hazard for the failure of bond strength.

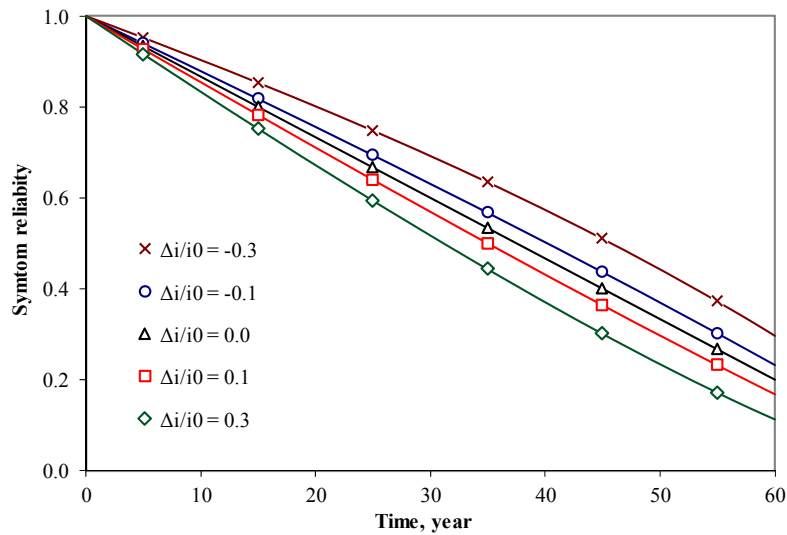


Fig. 14 Influence of measured corrosion rates on symptom reliability associated with bond strength evolution

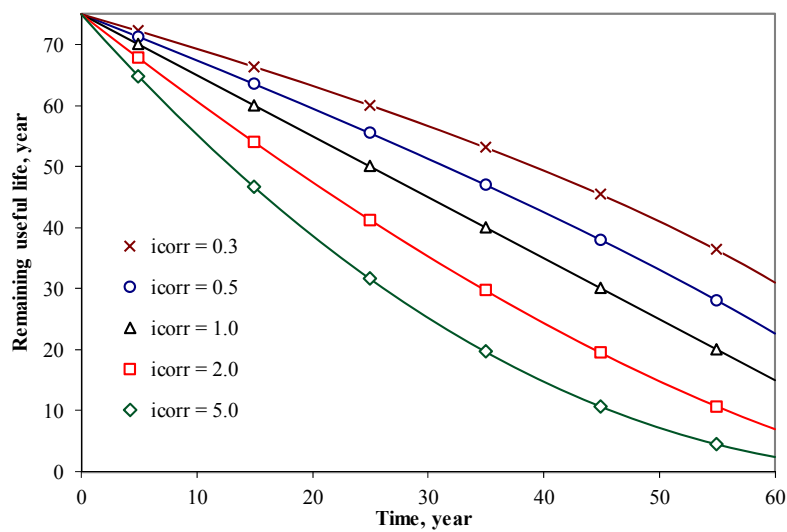


Fig. 15 Estimated remaining useful lifetimes associated with bond strength evolution over life time t for various corrosion rates rates

The corrosion rate in operational environments may be different from the corrosion rate used in concrete structural design. Therefore, it is necessary to adjust the reliability in operational environments on the basis of the corrosion rate measured on site. The results in Fig. 14 give the predictions of the associated symptom reliability for different values of corrosion rate change ($\Delta i/i_0$), ranging from -0.3 to +0.3. As expected, the associated symptom reliability increases if the field measurements of corrosion rate are below the expected value, and decreases if field measurements

on site increase.

From the obtained symptom reliability over time, the remaining useful life associated with bond strength deterioration can be predicted, as shown in Fig. 15. For the concrete structure concerned, the remaining useful life is 15 *year* after the structure served 60 years in the case with corrosion rate of $1.0 \mu\text{A}/\text{cm}^2$. The remaining life can be decreased when corrosion rate increases, reducing to 2.4 *year* if the concrete structure still survives after 60 year service in the case with corrosion rate of $5.0 \mu\text{A}/\text{cm}^2$.

6. Conclusions

On the basis of the results from the numerical example involving the reliability analyses for the concrete structures affected by reinforcement corrosion, the following conclusions are noted: 1) The proposed analytical models can correctly predict the concrete cracking growth and rebar bond strength deterioration induced by reinforcement corrosion during the residual life of corroded RC structures; 2) The concrete cracking development and bond strength evolution can be modelled as Weibull distribution with appropriate shape and scale parameters; 3) The symptom reliability associated with concrete cracking and bond strength evolution is significantly affected by the reinforcement corrosion rate, decreasing as the corrosion rate increases; 4) The symptom reliability could be adjusted from the real monitored corrosion rates to reflect the difference between the monitored data and the predicted results; 5) The remaining useful life largely depends on the corrosion rate, decreasing significantly as corrosion rate increases. The present research focuses on RC structural members from numerical simulations, but could be further extended to real complex RC structures.

References

- Bhargava, K., Ghosh, A.K., Mori, Y. and Ramanujam, S. (2007), "Corrosion-induced bond strength degradation in reinforced concrete: analytical and empirical models", *Nucl. Eng. Des.*, **237**, 1140-1157.
- Cairns, J., Du, Y. and Law, D. (2006), "Residual bond strength of corroded plain round bars", *Mag. Concrete Res.*, **58**(4), 221-231.
- Cempel, C., Natke, H.G. and Yao, J.T.P. (2000), "Symptom reliability and hazard for systems condition monitoring", *Mech. Syst. Sig. Proc.*, **14**(3), 495-505.
- Ceravolo, R., Pescatore, M. and De Stefano, A. (2009), "Symptom-based reliability and generalized repairing cost in monitored bridges", *Reliab. Eng. Syst. Saf.*, **94**(8), 1331-1339.
- Chen, H.P. and Alani, A.M. (2012), "Reliability and optimised maintenance for sea defences", *Proceedings of the ICE: Maritime Engineering*, **165**(2), 51-64.
- Chen, H.P. and Alani, A.M. (2013), "Optimized maintenance strategy for concrete structures affected by cracking due to reinforcement corrosion", *ACI Struct. J.*, **110**(2), 229-238.
- Chen, H.P. and Bicanic, N. (2010), "Identification of structural damage in buildings using iterative procedure and regularisation method", *Eng. Comput.*, **27**(8), 930-950.
- Chen, H.P. and Xiao, N. (2011), "Symptom-based damage prognosis for deteriorating bridge structures", *The 6th International Workshop on Advanced Smart Materials and Smart Structures Technology (ANCRiSST 2011)*, Dalian, China.
- Chen, H.P. and Xiao, N. (2012), "Analytical solutions for corrosion-induced cohesive concrete cracking", *J. Appl. Math.*, Article ID 769132, 25, doi:10.1155/2012/769132.
- Fang, C., Yang, S. and Zhang, Z. (2013), "Bending characteristics of corroded reinforced concrete beam

- under repeated loading”, *Struct. Eng. Mech.*, **47**(6), 773-790.
- Frangopol, D.M., Strauss, A. and Kim, S. (2008), “Use of monitoring extreme data for the performance prediction of structures: General approach”, *Eng. Struct.*, **30**(12), 3644-3653.
- Giuriani, E., Plizzari, G. and Schumm, C. (1991), “Role of stirrups and residual tensile strength of cracked concrete on bond”, *J. Struct. Eng.*, ASCE, **117**(1), 1-18.
- Kim, K., Bolander, J.E. and Lim, Y.M. (2012), “Simulation of corroded RC structures using a three-dimensional irregular lattice model”, *Struct. Eng. Mech.*, **41**(5), 645-662.
- Law, D.W., Tang, D., Molyneaux, T.K.C. and Gravina, R. (2011), “Impact of crack width on bond: confined and unconfined rebar”, *Mater. Struct.*, **44**, 1287-1296.
- Lawless, J.F. (1982), *Statistical Models and Methods for Lifetime Data*, Wiley, New York.
- Liu, Y. and Weyers, R.E. (1998), “Modelling the time-to-corrosion cracking in chloride contaminated reinforced concrete structures”, *ACI Mater. J.*, **95**(6), 675-681.
- Melchers, R.E. (1999), *Structural Reliability: Analysis and Prediction*, Chichester UK, John Wiley and Sons.
- Mullard, J.A. and Stewart, M.G. (2011), “Corrosion-induced cover cracking: new test data and predictive models”, *ACI Mater. J.*, **108**(1), 71-79.
- Nepal, J., Chen, H.P. and Alani, A.M. (2013), “Analytical modelling of bond strength degradation due to reinforcement corrosion”, *Key Eng. Mater.*, **569**, 1060-1067.
- Ortega, N.F., Rivas, I.E., Avelano, R.R. and Peralta, M.H. (2011), “Beams affected by corrosion influence of reinforcement placement in the cracking”, *Struct. Eng. Mech.*, **37**(2), 163-176.
- Pantazopoulou, S.J. and Papoulia, K.D. (2001), “Modelling cover cracking due to reinforcement corrosion in RC structures”, *J. Eng. Mech.*, ASCE, **127**(4), 342-351.
- Sadeghi, J. and Rezvani, F.H. (2013), “Development of non-destructive method of detecting steel bars corrosion in bridge decks”, *Struct. Eng. Mech.*, **46**(5), 615-627.
- Stewart, M.G. and Rosowsky, D.V. (1998), “Time-dependent reliability of deteriorating reinforced concrete bridge decks”, *Struct. Saf.*, **20**(1), 91-109.
- Straub, D. and Faber, M.H. (2005), “Risk based inspection planning for structural systems”, *Struct. Saf.*, **27**(4), 335-355.
- Torres-Acosta, A.A. and Martinez-Madrid, M.M. (2003), “Residual life of corroding reinforced concrete structures in marine environment”, *J. Mater. Civil Eng.*, ASCE, **15**(4), 344-353.
- Vidal, T., Castel, A. and Francois, R. (2004), “Analyzing crack width to predict corrosion in reinforced concrete”, *Cement Concrete Res.*, **34**(1), 165-174.